Title

Association between urinary per- and poly-fluoroalkyl substances and COVID-19 susceptibility

Authors

Ji, Junjun

Song, Lingyan

Wang, Jing

et al.

Publication Date

2021-08-01

DOI

10.1016/j.envint.2021.106524

Since January 2020 Elsevier has created a COVID-19 resource centre with free information in English and Mandarin on the novel coronavirus COVID-19. The COVID-19 resource centre is hosted on Elsevier Connect, the company's public news and information website.

Environment International 153 (2021) 106524

Contents lists available at ScienceDirect

Environment International

journal homepage: www.elsevier.com/locate/envint

Association between urinary per- and poly-fluoroalkyl substances and COVID-19 susceptibility

Junjun Ji [a,b,1], Lingyan Song [c,1], Jing Wang [d,1], Zhiyun Yang [e], Haotian Yan [f], Ting Li [a], Li Yu [g,h], Lingyu Jian [e], Feixiang Jiang [b], Junfeng Li [a,*], Jinping Zheng [i,*], Kefeng Li [h,*]

[a] Department of Radiology, Heping Hospital Affiliated to Changzhi Medical College, Changzhi, Shanxi, China
[b] Jiangsu Metabo Life Technology, Danyang, Jiangsu, China
[c] Department of Clinical Laboratory, Heping Hospital Affiliated to Changzhi Medical College, Changzhi, Shanxi, China
[d] Department of Critical Care Medicine, Yantai Yuhuangding Hospital Affiliated with Medical College of Qingdao University, Yantai, Shandong, China
[e] Graduate School, Changzhi Medical College, Changzhi, Shanxi, China
[f] Peking University First Hospital, Beijing, China
[g] Department of Oncology, Shengjing Hospital of China Medical University, Shenyang, China
[h] School of Medicine, University of California, San Diego, CA, USA
[i] School of Public Health and Preventive Medicine, Changzhi Medical College, Changzhi, Shanxi, China

ARTICLE INFO

Handling Editor: Heather Stapleton

Keywords:
Per- and poly-fluoroalkyl substances
COVID-19
Susceptibility
Metabolic abnormalities
Urine

ABSTRACT

Background and Objective: The growing impact of the COVID-19 pandemic has heightened the urgency of identifying individuals most at risk of infection. Per- and poly-fluoroalkyl substances (PFASs) are manufactured fluorinated chemicals widely used in many industrial and household products. The objective of this case-control study was to assess the association between PFASs exposure and COVID-19 susceptibility and to elucidate the metabolic dysregulation associated with PFASs exposure in COVID-19 patients.

Methods: Total 160 subjects (80 COVID-19 patients and 80 symptom-free controls) were recruited from Shanxi and Shandong provinces, two regions heavily polluted by PFASs in China. Twelve common PFASs were quantified in both urine and serum. Urine metabolome profiling was performed by liquid chromatography coupled with tandem mass spectrometry (LC-MS/MS).

Results: In unadjusted models, the risk of COVID-19 infection was positively associated with urinary levels of perfluorooctanesulfonic acid (PFOS) (Odds ratio: 2.29 [95% CI: 1.52–3.22]), perfluorooctanoic acid (PFOA) (2.91, [1.95–4.83], and total PFASs ($\sum$ (12) PFASs) (3.31, [2.05–4.65]). After controlling for age, sex, body mass index (BMI), comorbidities, and urine albumin-to-creatinine ratio (UACR), the associations remained statistically significant (Adjusted odds ratio of 1.94 [95% CI: 1.39–2.96] for PFOS, 2.73 [1.71–4.55] for PFOA, and 2.82 [1.97–3.51] for $\sum$ (12) PFASs). Urine metabolome-PFASs association analysis revealed that 59% of PFASs-associated urinary endogenous metabolites in COVID-19 patients were identified to be produced or largely regulated by mitochondrial function. In addition, the increase of PFASs exposure was associated with the accumulation of key metabolites in kynurenine metabolism, which are involved in immune responses (Combined β coefficient of 0.60 [95% CI: 0.25–0.95, $P = 0.001$]). Moreover, alternations in PFASs-associated metabolites in mitochondrial and kynurenine metabolism were also correlated with clinical lab biomarkers for mitochondrial function (serum growth/differentiation factor-15) and immune activity (lymphocyte percentage), respectively.

Conclusion: Elevated exposure to PFASs was independently associated with an increased risk of COVID-19 infection. PFASs-associated metabolites were implicated in mitochondrial function and immune activity. Larger studies are needed to confirm our findings and further understand the underlying mechanisms of PFASs exposure in the pathogenesis of SARS-CoV2 infection.

* Corresponding authors at: Department of Radiology, Heping Hospital Affiliated to Changzhi Medical College, 110 Yan'an S Rd, Changzhi, Shanxi, China (J. Li). School of Public Health and Preventive Medicine, Changzhi Medical College, Jiefang E St, Changzhi, Shanxi, China (J. Zheng). School of Medicine, University of California, San Diego, 9500 Gilman Dr, La Jolla, CA 92093, USA (K. Li).
E-mail addresses: lijunfeng@czmc.edu.cn (J. Li), zhengjp@czmc.edu.cn (J. Zheng), kli@ucsd.edu (K. Li).
[1] These authors contributed equally to this work.

https://doi.org/10.1016/j.envint.2021.106524
Received 27 September 2020; Received in revised form 9 March 2021; Accepted 11 March 2021
Available online 19 March 2021

1. Introduction

The coronavirus disease 2019 (COVID-19) caused by severe acute respiratory syndrome coronavirus 2 (SARS-CoV-2) has rapidly evolved into a global pandemic after its first report in Wuhan, China, in December 2019 (Zhu et al., 2020). There is clear evidence of high heterogeneity in COVID-19 susceptibility (probability of being infected) (Viner et al., 2020). The growing impact of the pandemic intensifies the need for identifying individuals most at risk of infection. Such information will not only be useful for public health experts, but also for individuals seeking to assess their own personalized risk. Prior studies have hypothesized that differences in COVID-19 susceptibility are associated with age (Liu et al., 2020), sex (Haitao et al., 2020), BMI (Jung et al., 2020), genetic factors (Anastassopoulou et al., 2020) and certain comorbidities such as obesity, type 2 diabetes, cardiovascular diseases (CVDs) (Aung et al., 2020). However, COVID-19 is a new disease, and more work is urgently needed to determine if there are other factors that increase a person's risk to contract the infection. Little information is available regarding the impact of environmental exposures on COVID-19 susceptibility.

Per- and poly-fluoroalkyl substances (PFASs) are synthetic chemicals containing fluorinated carbon chains with different functional groups. Due to their excellent thermal and chemical stability, hydrophobic and oleophobic properties, PFASs have been widely used as coatings in many consumer products such as disposable food packaging, cookware, carpets, furniture, and more (Susmann et al., 2019). The widespread use of PFASs has resulted in the ubiquitous detection of these chemicals in various environments, including drinking water, air, soil, crops, seafood, and wildlife (Li et al., 2019; Liu et al., 2019; Wang et al., 2020). Depending on the perfluoroalkyl chain length and trophic position, some PFASs species such as perfluorooctanoic acid (PFOA) and perfluorooctanesulfonic acid (PFOS) have long biological half-lives (3.5 years for PFOA and 4.8 years for PFOS in humans) (Perez et al., 2013). It was reported that over 85% of people in the United States and China have detectable PFOS and PFOA in their blood (Li et al., 2013; Pan et al., 2010; Pelch et al., 2019; Tian et al., 2018).

Epidemiological studies have indicated that PFASs exposure is linked to the increased risks of cancer, liver damage, and diabetes (McGlinchey et al., 2020; Pelch et al., 2019). Additionally, toxicological studies underscore the immunotoxic potential of PFASs, which may adversely affect the immune responses to infectious diseases and vaccination (Chang et al., 2016; DeWitt et al., 2019; Zeng et al., 2019). For instance, several studies found that exposure to PFASs was associated with increased risks of respiratory tract infections, otitis media, respiratory syncytial virus (RSV), and pneumonia (Ait Bamai et al., 2020; Granum et al., 2013; Impinen et al., 2018). Decreased antibody responses to booster, measles, mumps, and rubella (MMR) vaccination had also been observed in individuals exposed to PFASs (Grandjean et al., 2012; Kielsen et al., 2016; Timmermann et al., 2017).

Metabolites in biological fluids are the intermediate or end products of metabolism, which may reflect the final consequences of the functional changes in response to external exposures (Oresic et al., 2020). Identifying these metabolic changes by next-generation metabolomics might provide insights into the mechanisms underlying exposure-related diseases (Han et al., 2018). Regarding PFASs, the recent metabolomic analysis revealed that PFASs exposure might cause metabolic perturbations in phospholipid and amino acid metabolism, thereby contributing to increased risk and pathogenesis of diabetes and other metabolic disorders (Alderete et al., 2019; Kingsley et al., 2019; McGlinchey et al., 2020). In addition, metabolites play important roles in the pathogenesis of infectious diseases and host immune responses. On the one hand, small molecules from the host metabolism are essential for viral infection and replication because they provide building blocks that a rapidly proliferating virus requires to assemble its nucleic acids, proteins (including capsid proteins), and membrane (Gonzalez Plaza et al., 2016; Thomas et al., 2020). Dysregulation of amino acid metabolism, tricarboxylic acid cycle (TCA) and fatty acid oxidation had been characterized in patients with RSV and dengue virus infection (Shahfiza et al., 2017; Turi et al., 2018). In a recent study, COVID-19 infection was reported to be associated with increased tryptophan catabolism (Thomas et al., 2020). On the other hand, metabolites such as organic acids, short-chain fatty acids, bile acids, and tryptophan metabolites fuel and regulate the maturation of immune responses (Ganeshan and Chawla 2014; Michaudel and Sokol 2020). Collectively, results from these studies suggested that PFASs exposure might be associated with perturbations in metabolic pathways which are implicated in viral infection.

In this cohort study of 160 participants from two regions with high PFASs pollution in China, we, (i) quantified urinary levels of PFASs in these subjects and examined the associations between PFASs exposure and COVID-19 infection, (ii) conducted metabolomic analysis to examine the metabolic differences in urine metabolome between symptom-free controls, and COVID-19 patients, (iii) performed a metabolome-wide association study coupled with pathway enrichment analysis to find out the metabolic abnormities in COVID-19 patients associated with urinary PFASs concentrations (Fig. 1a for the experiment design). We hypothesized that PFASs exposure would be associated with alternations in key metabolic pathways involved in mitochondrial metabolism and immune responses, which may be associated with increased COVID-19 risk.

2. Materials and methods

The brief methods were described below, and the details can be found in the supplemental materials.

2.1. Subjects recruitment

COVID-19 patients were recruited from January 7, 2020 to March 5, 2020 in Shanxi and Shandong, two provinces with high PFASs exposure and incidence of COVID-19 in China (Liu et al., 2019; Xie et al., 2013; Zhang et al., 2020a). Details regarding PFASs and incidence of COVID-19 in Shandong and Shanxi provinces were described in Supplemental Methods. The diagnosis of COVID-19 was made by SARS-CoV-2 nucleic acid testing of nasopharyngeal swabs in the COVID-19 testing centers at Heping Hospital Affiliated to Changzhi Medical College, Shanxi, and Yantai Yuhuangding Hospital, Shandong. COVID-19 disease severity was judged according to the guidelines for the diagnosis and management of COVID-19 patients (7th edition) by the National Health Commission of China. All COVID-19 patients in our study had mild clinical symptoms such as fever, fatigue, dry cough, muscle pain, and sore throat, and no signs of pneumonia on chest CT imaging. They were quarantined and given general supportive treatment including bed rest, adequate nutrition, water and electrolyte balance, and intensively monitoring of vital signs.

SARS-CoV-2 negative controls were recruited from the aggressive contact tracing for all potential contacts of the confirmed COVID-19 patients, which is part of the authorities' COVID-19 surveillance (Xing et al., 2020). The selected controls were age, sex, and location matched with the COVID-19 patients. None of the controls had COVID-19-related symptoms.

Finally, 160 participants were recruited, including 80 (40 COVID-19 patients and 40 controls) from Shanxi and 80 subjects from Shandong (40 COVID-19 patients and 40 controls). The baseline characteristics of the subjects are listed in Table 1. The study protocol was approved by the Institutional Review Boards (IRBs) of Changzhi Medical College (IRB#: CZMC20200231) and Yantai Yuhuangding Hospital (Approved No. 202011). Written informed consent was obtained from all the subjects.

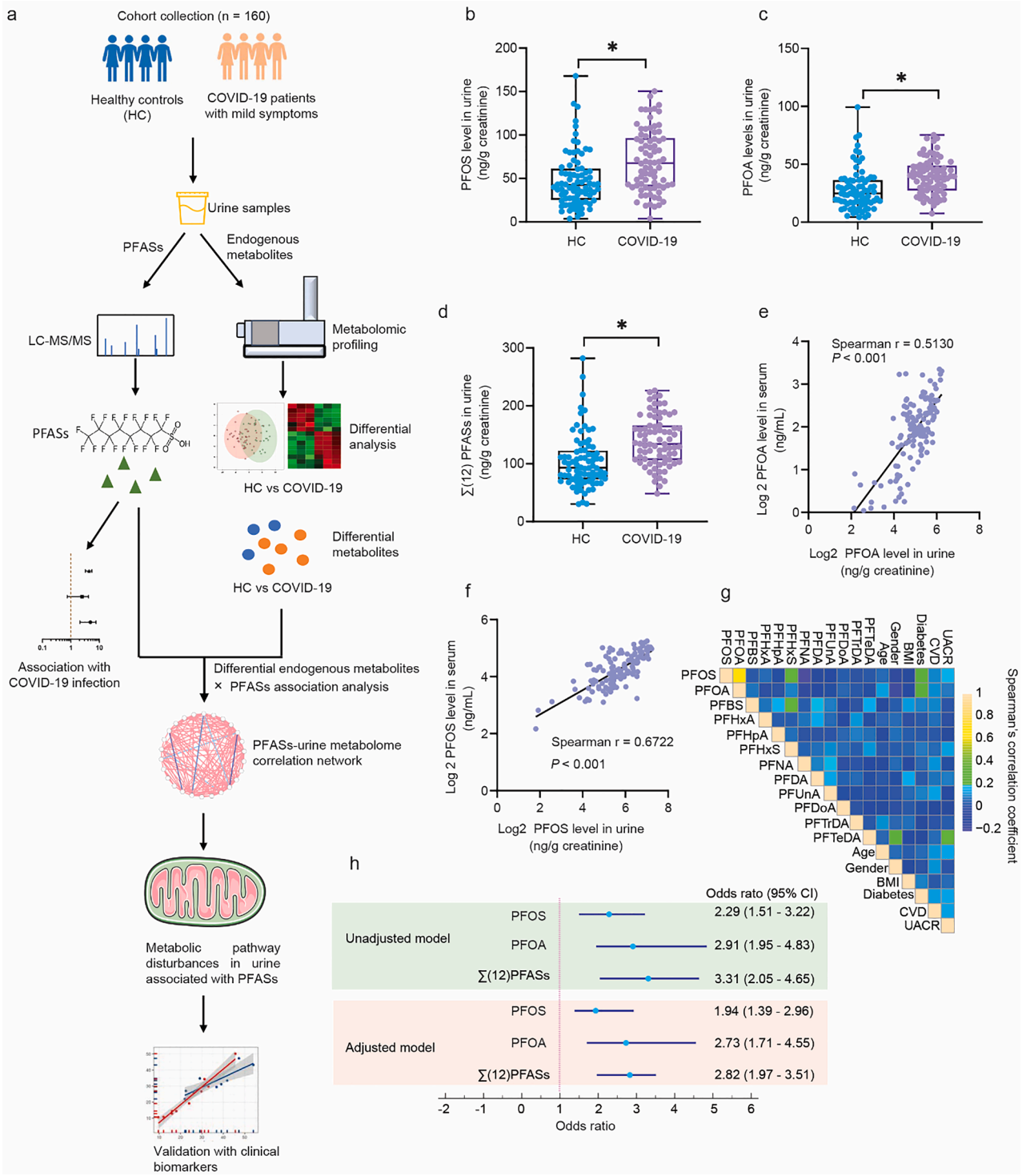

Fig. 1. Elevated exposure of perfluorinated alkyl substances (PFASs) is significantly associated with higher risks of SARS-CoV-2 infection. (a) An illustration of the experimental design. Total 160 subjects were enrolled including 80 infected healthy controls (HC), and 80 COVID-19 patients. All CVOD-19 patients in our analysis had mild clinical symptoms such as fever, fatigue, dry cough, muscle pain and sore throat and no signs of pneumonia on chest CT imaging. (b-d) The urinary concentration (ng/g creatinine) of PFOS (b), PFOA (c), and total PFASs (d) in HC (n = 80), and COVID-19 patients (n = 80). The box-whisker plots show the medians (middle line) and the first and third quartiles (boxes), whereas the whiskers are the maximum and minimum values. Mann-Whitney *U* test was performed. $^*P < 0.05$. (e) PFOA levels in urine were significantly correlated with levels in serum. Data were log 2 transformed, and Spearman's rank correlation was performed. (f) PFOS levels in urine correlated with levels in serum. Data were log 2 transformed, and Spearman's rank correlation was performed. (g) Correlation plot of PFASs and clinical characteristics. Spearman's rank-order correlation was conducted, and Spearman's correlation coefficients were plotted. (h) The associations between PFASs exposure and COVID-19 infection using unadjusted and multivariable adjusted models. PFASs values were log 2 transformed before regression analysis. Odds ratios represent the risks of COVID-19 infection per log 2 standard deviation (SD) of urinary PFASs increment. Log 2 SD was 1.02, 0.93, and 0.62 ng/g urinary creatinine, for PFOS, PFOA, and total PFASs, respectively. The multiple logistic models were adjusted for potential covariates including age, gender, body mass index (BMI), diabetes, cardiovascular diseases (CVDs), and urine albumin-to-creatinine ratio (UACR). Abbreviations: PFASs: Perfluorinated alkyl substances; 95% CI: 95% confidence interval.

Table 1
Summary of characteristics of the study participants.

Characteristic	HC (n = 80)	COVID-19 (n = 80)	*P* value
Age, years	50.3 ± 9.65	53.4 ± 8.99	0.251
Gender			1.00
Female, n (%)	38 (47.5%)	38 (47.5%)	
Male, n (%)	42 (52.5%)	42 (52.5%)	
BMI (kg/m^2)	24.0 ± 4.20	24.4 ± 4.10	0.778
COVID-19 symptoms before sample collection (Days)	N/A	2 (0–4)	N/A
Comorbidities, n (%)			
Diabetes	8 (10.0%)	9 (11.3%)	0.999
Cancer	0 (0%)	0 (0%)	1.00
Chronic kidney disease	0 (0%)	0 (0%)	1.00
Cardiovascular diseases (CVDs)	7 (8.75%)	8 (10.0%)	0.999
SARS-CoV-2 RNA in urine, n (%)	0 (0%)	0 (0%)	1.00
Urine WBC, n (%)			0.999
<5/hpf	77 (96.3%)	76 (95.0%)	
≥5/hpf	3 (3.75%)	4 (5.00%)	
Urine RBC, n (%)			0.999
<5/hpf	78 (97.5%)	79 (98.8%)	
≥5/hpf	2 (2.50%)	1 (1.25%)	
UACR (mg/g)			0.999
<30	77 (96.3%)	76 (95.0%)	
≥30	3 (3.75%)	4 (5.00%)	

The continuous variables are mean and standard deviations (mean ± SD) or median and interquartile range (IQR). The categorical characteristics are described as numbers (%). Differences between groups were analyzed by Student's *t* test, Mann-Whitney *U* test or chi-square test (compare the proportions). All CVOD-19 patients had mild clinical symptoms such as fever, fatigue, dry cough, muscle pain and sore throat and no signs of pneumonia on chest CT imaging. Abbreviations: HC: Healthy control; BMI: Body mass index; WBC: White blood cell; hpf: High power field; RBC: Red blood cell; UACR: urine albumin-to-creatinine ratio.

2.2. Biofluid sample collection

Paired blood and morning urine samples were collected after the subjects were tested positive or negative for SARS-CoV-2. Urine samples were collected and centrifuged at 1500*g* for 10 min to remove any cellular debris. Whole blood samples were drawn in lithium heparin tubes. Additionally, blood samples were collected into 4 mL BD vacutainer serum separator tubes (SSTs) for serum. Serum was obtained by allowing whole blood to coagulate for 30 min at room temperature before centrifugation at 1500*g* for 10 min at 4 °C. All whole blood samples were refrigerated until analyzed. Urine and sera samples were aliquoted into screw-capped cryovials and stored at −80 °C before analysis.

2.3. Routine blood and urine analysis

Lymphocyte percentage (LYP, %) in whole blood samples was analyzed using an automated hematology analyzer XE-5000 (Sysmex, Japan). Serum growth and differentiation factor 15 (GDF-15) was quantified using human GDF-15 ELISA kits (Abcam, CA, USA) according to the manufacturer's instructions. Urinary creatinine was measured based on a modified Jaffe reaction using urinary creatinine assay kits obtained from Cayman Chemical (MI, USA). Urinary albumin was determined by the immunoturbidimetry method using human albumin ELISA kits (Abcam, CA, USA). The value of the albumin-to-creatinine ratio (UACR) was obtained by calculating the ratio of urinary albumin (mg) to urinary creatinine (g).

2.4. Determination of PFASs in urine and serum

Samples from Shandong were shipped to Changzhi Medical College in Shanxi province for PFASs quantification and metabolomic analysis. Sample extraction and analysis for PFASs were performed as described previously (McGlinchey et al., 2020). Briefly, PFASs in urine and serum was extracted with methanol-acetonitrile (1:1, v/v) containing isotopically labeled internal standards (Table S1). The extract was analyzed on a Shimadzu LC-20A ultra-high-performance liquid chromatography coupled with SCIEX QTRAP 6500+ triple quadrupole mass spectrometer (LC-MS/MS) according to U.S. EPA method 537.1 with modifications. In total, 12 common PFASs were targeted by scheduled multiple reaction monitoring (sMRM) (Table S1). The concentrations of PFASs were calculated by peak area ratios between the analytes and internal standards. The total PFASs in urine and serum was calculated using the molar sum method. Urine PFASs were further normalized using the urinary creatinine (expressed as ng/g creatinine). Serum PFASs were expressed as ng/mL. We had only 52 serum samples for the controls and these samples were used to analyze the correlations between serum PFASs and urinary PFASs.

2.5. Urine metabolomic analysis

The extraction and metabolomic profiling of urine endogenous metabolites were performed as described before with minor modifications for the column length (Yuan et al., 2012). Method details were described in the supplemental materials. Briefly, metabolites in urine were extract with four volumes of prechilled (−20 °C) extraction buffer containing methanol and acetonitrile (50:50, v/v). Metabolomic analysis of 462 metabolites from 63 metabolic pathways was performed by LC-MS/MS. Chromatographic separation was conducted on a 100 mm × 4.6 mm, 3.5 μm XBridge amide column (Waters, USA) held at 25 °C. A total of 330 of the 462 targeted metabolites were measurable in all urine samples. Metabolomic data were normalized using urinary creatinine concentration for comparative analysis (Khamis et al., 2018). The quality control and analytical performance were described in the supplemental materials.

2.6. Statistical analysis

The continuous variables are mean ± standard deviation (SD) or as the median and interquartile range (IQR) (Skewed data). The categorical characteristics are described as numbers (%). PFASs levels were log2 transformed prior to statistical analysis. Missing data due to lower limit of detection (LLOD) were estimated using multiple imputation (m = 5) in IVEware v0.3 and replaced with random values between 0 and LLOD with the same probabilistic distribution of the observed PFASs concentrations (Table 2 for the detection rate of PFASs) (Harel et al., 2014; Lubin et al., 2004). Differences for continuous variables between controls, and COVID-19 patients were analyzed using either Student's *t* test or Mann–Whitney *U* test (Skewed data). The categorical data were analyzed using chi-square test. $P < 0.05$ was statistically significant. The relationship between PFASs in serum and the matched urine samples was calculated using Spearman's rank order correlation.

PFASs levels were log 2 transformed and standardized by z-scores before regression analysis. The logistic regression analyses were performed on COVID-19 patients (all mild cases) and controls to examine the associations between urinary PFASs and COVID-19 susceptibility. Both univariate and multivariate models were used to calculate odds ratios and 95% confidence intervals (CIs) of COVID-19 susceptibility associated with a 1-SD increment in PFASs levels (ng/g creatinine). Confounding factors for inclusion in multivariable models were selected based on univariable logistic regression analysis ($P < 0.1$), correlations with PFASs or the evidence from the literature (Liu et al., 2020). Finally, age, gender, body mass index (BMI), diabetes, cardiovascular diseases (CVDs), and kidney health biomarker UACR were included in the

Table 2
The detection frequency and concentrations of PFASs in urine.

PFASs	Acronym	Detection rate, n (%)			Urinary levels (median and IQR) (ng/g creatinine)		
		HC (n = 80)	COVID-19 (n = 80)	*P* value	HC (n = 80)	COVID-19 (n = 80)	*P* value
Perfluorooctanesulfonic acid	PFOS	80 (100%)	80 (100%)	1.00	42.4 (25.5–61.3)	67.6 (41.0–96.5)	<0.05
Perfluorooctanoic acid	PFOA	80 (100%)	80 (100%)	1.00	24.8 (16.9–36.3)	39.6 (27.5–48.9)	<0.05
Perfluorobutane sulfonic acid	PFBS	35 (43.8%)	34 (42.5%)	0.90	5.11 (4.40–6.50)	5.51 (4.21–6.93)	0.51
Perfluorohexanoic acid	PFHxA	4 (5.00%)	3 (3.75%)	1.00	0.366 (0.29–0.41)	0.344 (0.259–0.403)	0.86
Perfluoroheptanoic acid	PFHpA	10 (12.5%)	11 (13.8%)	1.00	2.56 (1.85–5.31)	4.3 (2.45–6.64)	0.43
Perfluorohexane sulfonic acid	PFHxS	69 (86.3%)	65 (81.3%)	0.52	12.8 (18.6–42.9)	22.1 (15.0–37.7)	0.18
Perfluorononanoic acid	PFNA	41 (51.3%)	39 (48.8%)	0.88	8.19 (7.14–9.08)	8.57 (7.45–10.6)	0.21
Perfluorodecanoic acid	PFDA	46 (57.5%)	44 (55.0%)	0.87	9.23 (7.52–12.0)	11.7 (8.64–14.0)	0.051
Perfluoroundecanoic acid	PFUnA	33 (41.2%)	31 (38.8%)	0.87	3.91 (3.28–5.25)	4.60 (3.90–6.10)	0.069
Perfluorododecanoic acid	PFDoA	7 (8.75%)	6 (7.50%)	1.00	0.873 (0.831–1.10)	0.945 (0.845–1.05)	0.98
Perfluorotridecanoic acid	PFTrDA	6 (7.50%)	7 (8.75%)	1.00	0.721 (0.546–0.791)	0.831 (0.653–1.00)	0.37
Perfluorotetradecanoic acid	PFTeDA	5 (6.25%)	4 (5.00%)	1.00	0.061 (0.047–0.074)	0.077 (0.053–0.089)	0.35

Detection frequencies are presented as n (%). The levels of PFASs in urine are listed as median and interquartile range (IQR). Chi-square analysis was performed for group differences of detection frequencies. Urinary levels of PFASs between HC and COVID-19 were compared using Mann–Whitney U tests. All CVOD-19 patients had mild clinical symptoms such as fever, fatigue, dry cough, muscle pain and sore throat and no signs of pneumonia on chest CT imaging. The lower limit of detection (LLOD) levels of PFOS, PFOA, PFBS and PFHxA were 0.01 ng/g creatinine in urine. Other PFASs had LLOD levels of 0.02 ng/g creatinine in urine. Abbreviations: PFASs: Perfluorinated alkyl substances; HC: Healthy controls.

multivariable model.

Metabolomic data were log2 transformed before metabolomic analysis. Partial least squares discriminant analysis (PLS-DA) was performed in MetaboAnalyst 5.0. The validation of the PLS-DA model was performed via the leave-one-out cross-validation (LOOCV) method. Metabolites with PLS-DA variable importance in projection (VIP) scores >1.5 were statistically significant. Metabolic pathway analysis was performed using a custom Python script with an in-house library for human metabolism. The associations between PFASs and urinary endogenous metabolites were evaluated using correlation network analysis with Spearman's rank correlation in Cytoscape 3.8.2. The correlation threshold was set as 0.2, *P* value <0.05 and false discovery rate (FDR) <20%. We also performed the multiple linear regression analysis to further confirm the associations between the exposure of PFASs and changes in metabolism. The effect sizes (Beta) and *P* values were adjusted for confounders described in the multivariate logistic regression model. The summary effect of PFASs exposure on a metabolic pathway was meta-analyzed using the random-effects model. Spearman's rank correlation was conducted to determine the correlations between metabolite levels and clinical laboratory markers of mitochondrial metabolism (serum GDF-15) and immune function (lymphocyte percentage, %).

All general statistical analyses were performed in GraphPad Prism 9.0 (San Diego, CA) unless specified in the methods and legends.

3. Results

3.1. PFASs concentrations in urine of COVID-19 patients and symptom-free controls

All the participants in this study are Chinese from Shanxi (n = 80) and Shandong (n = 80) provinces. None of them worked in higher-risk COVID-19 occupations such as frontline workers or occupational workers in fluorochemical plants. The urinary PFASs levels in the subjects from Shandong were not statistically different from those in the subjects from Shanxi (Fig. S1). The characteristics of the participants for symptom-free healthy controls (n = 80) and COVID-19 patients (n = 80) are shown in Table 1. The average (±SD) age was 50.3 (±9.65) for HC and 53.4 (±8.99) for COVID-19 patients. We did not observe significant differences in age, gender, and BMI between HC and COVID-19 patients. The proportions of subjects with diabetes, and CVDs in HC did not differ from those in COVID-19 patients. The median time with mild COVID-19 symptoms before COVID-19 testing and sample collection was 2 days (IQR: 0–4). The brief experiment design for this study is shown in Fig. 1a.

We first quantified the urinary levels of PFASs in all the samples by LC-MS/MS. The targeted PFASs compounds, their retention times (RTs), and MS/MS parameters are listed in Table S1. Out of 12 PFASs measured, perfluorooctanesulfonic acid (PFOS) and perfluorooctanoic acid (PFOA) were detected in the urine samples of all participants (Table 2). Other PFASs were detected in 5.00%−86.3% of HC samples, and the detection frequency was not statistically different between HC and COVID-19 groups (all $P > 0.05$) (Table 2).

The urinary levels of PFASs and total PFASs ($\sum$ (12) PFASs) in HC and COVID-19 patients are shown in Fig. 1b−d and Table 2. PFOS and PFOA are the dominant PFASs in the urine samples of our cohort. Among the detected PFASs, PFOS showed the highest urinary concentration, with a median level of 42.4 ng/g creatinine (IQR: 25.5–61.3 ng/g creatinine) in controls and 67.6 ng/g creatinine (IQR: 42.5–103.7) in COVID-19 patients ($P < 0.05$) (Fig. 1b). Similarly, COVID-19 patients had significantly higher median levels of PFOA and total PFASs in urine than those in symptom-free controls ($P < 0.05$) (Fig. 1c and d).

3.2. Correlations between urinary and serum PFASs, and baseline clinical characteristics

Correlations between urinary and serum PFOS and PFOA levels: Previous animal studies have demonstrated that urine was the primary elimination route for PFOA and PFOS in rats (Cui et al., 2010). We then analyzed the correlations between urinary levels of PFOS and PFOA and their corresponding serum concentrations. The median serum PFOS was 19.1 ng/mL (IQR: 14.4–26.1) and the median serum PFOA was 3.87 ng/mL (IQR: 2.97–5.32) A good correlation was observed for PFOA between urine and serum concentrations (Spearman's correlation coefficient r = 0.51, $P < 0.001$) (Fig. 1e). PFOS levels in urine were also significantly correlated with concentrations in serum (Spearman's correlation coefficient r = 0.67, $P < 0.001$) (Fig. 1f). These results suggested that urinary PFASs might be good indicators of the internal dose and used for evaluating human exposure to PFASs.

Correlations between urinary PFASs and baseline clinical characteristics: Different urinary PFASs showed moderate to strong pairwise correlations, with the strongest correlation observed between PFOA and PFOS (Spearman's correlation coefficient r = 0.73) (Fig. 1g). We also found a weak correlation between PFOA and gender (Spearman r = −0.22, $P < 0.05$) (Fig. 1f). Females tend to have lower levels of PFOA and PFOS than those in males. In addition, the number of subjects with diabetes was positively correlated with urinary PFOS and PFOA levels.

3.3. Associations between urinary PFASs and COVID-19 susceptibility

We next evaluated the associations between PFASs exposure and COVID-19 infection using both unadjusted and multivariate adjusted models.

Unadjusted models: In unadjusted analyses, PFOS, PFOA, and ∑ (12) PFASs were generally associated with COVID-19 susceptibility [odds ratio of 2.29 (95% CI: 1.52–3.22) for PFOS, 2.91 (1.95–4.83) for PFOA, and 3.31 (2.05–4.65) for ∑ (12) PFASs] (Fig. 1h).

Adjusted models: Confounding factors including age, gender, BMI, and diabetes were selected for adjusted models based on univariate logistic regression analysis ($P < 0.1$), or Spearman's rank correlations with urinary PFASs ($P < 0.05$). Urine albumin-to-creatinine ratio (UACR) is a well-documented biomarker for renal function (Lopez-Giacoman and Madero 2015). Since renal function may affect the excretion of PFASs (Lin et al., 2021), we also added UACR in the adjusted models. The adjusted associations of PFASs exposure with COVID-19 susceptibility are presented in Fig. 1h and Table 3. After controlling for age, sex, BMI, diabetes, CVDs and UACR, the associations between PFOS, PFOA and ∑ (12) PFASs and risk of COVID-19 infection remained statistically significant [Adjusted odds ratio of 1.94 (95% CI: 1.39–2.96) for PFOS, 2.73 (95% CI: 1.71–4.55) for PFOA, and 2.82 (95% CI: 1.97–3.51) for ∑ (12) PFASs] (Fig. 1h). Other PFASs were not significantly associated with COVID-19 susceptibility after adjustment for confounders (Table 3).

3.4. Identification of differential metabolites in urine between control and COVID-19 patients

We then performed metabolomic analysis to explore the differences in urine metabolome between control and COVID-19 patients. Out of 462 metabolites targeted, 335 were detected in all samples. The median intra-day and inter-day coefficient of variation (CVs) of metabolomics quality control (QC) samples were 10.2% and 11.5%, respectively, which indicated excellent reproducibility for the measured metabolites (Supplemental materials and methods).

Metabolomic profiling, followed by multivariate PLS-DA, revealed dramatic metabolic differences in urine metabolome between HC and COVID-19 patients (Fig. 2a). Since PLS-DA is a supervised model, we further verified the reliability of the PLS-DA model using the leave-one-out cross-validation (LOOCV) method (Fig. S2). Variable importance in projection (VIP) analysis showed the significant discriminating urinary metabolites between the control and COVID-19 group. The top 25 discriminating metabolites are shown in Fig. 2, and the full list of 54 differential metabolites between the two groups is in Table S2. For example, urinary metabolites of prostaglandins (PGF2 alpha, tetranor-PGEM, and 11-dTxB2) from eicosanoid metabolism were significantly increased in COVID-19 patients. In addition, patients with COVID-19 had higher levels of indolelactic acid, succinic acid, aconitic acid, and itaconic acid than those in controls, which are intermediates in mitochondrial metabolism. Urinary ceramides and metabolites in kynurenine pathways (L-Kynurenine and hydroxykynurenine) were also increased in COVID-19 patients. However, sphingomyelins (SM(d18:1/12:0) and nucleotide-related metabolites (Cyclic AMP) decreased dramatically in COVID-19 patients. Metabolomic characterization of sera and plasma identified similar metabolic abnormalities in COVID-19 patients (Shen et al., 2020; Thomas et al., 2020).

Table 3
The adjusted associations between urinary PFASs other than PFOS and PFOA with COVID-19 susceptibility.

PFASs	Acronym	COVID-19 susceptibility	
		Adjusted odds ratio (95% CI)	*P* value
Perfluorobutane sulfonic acid	PFBS	1.00 (0.523–1.939)	0.983
Perfluorohexanoic acid	PFHxA	0.605 (0.107–3.059)	0.543
Perfluoroheptanoic acid	PFHpA	1.123 (0.431–2.955)	0.811
Perfluorohexane sulfonic acid	PFHxS	1.071 (0.866–1.322)	0.548
Perfluorononanoic acid	PFNA	0.916(0.479–1.747)	0.791
Perfluorodecanoic acid	PFDA	0.938(0.485–1.811)	0.848
Perfluoroundecanoic acid	PFUnA	0.936(0.479–1.820)	0.844
Perfluorododecanoic acid	PFDoA	0.941(0.272–3.192)	0.921
Perfluorotridecanoic acid	PFTrDA	1.095(0.333–3.677)	0.881
Perfluorotetradecanoic acid	PFTeDA	0.817 (0.196–3.093)	0.767

PFASs with detection rate ≤ 50% were treated as categorical/binary exposure variable (Detected or non-detected) in the multiple logistic regression models (PFBS, PFHxA, PFHpA, PFNA, PFDA, PFUnA, PFDoA, PFTrDA, and PFTeDA. PFHxS (Detection rate ≥ 80%) was treated as continuous variable for logistic regression analysis. The level of PFHxS was log2 transformed and z score was then calculated using log2 transformed values before logistic regression. Odds ratios and 95% confidence intervals (CIs) for PFHxS represent the risks of SARS-CoV-2 infection (susceptibility) per standard deviation (SD) of PFHxS increment (ng/g urinary creatinine).The multiple logistic regression models were adjusted for potential covariates including age, gender, body mass index (BMI), diabetes, cardiovascular diseases (CVDs), and urine albumin-to-creatinine ratio (UACR).

3.5. Urine metabolic signatures associated with PFASs exposure in COVID-19 patients

Correlation network analysis was then conducted to identify what metabolic alterations in urine metabolome of COVID-19 patients were associated with PFASs exposure. Out of 54 differential urinary metabolites in COVID-19 patients (HC versus COVID-19) (Table S2), 49 were significantly correlated with urine concentrations of PFOA, PFOS, and ∑ (12) PFASs at coefficient r > 0.2 or <−0.2, FDR ≤ 20%, and $P < 0.05$ (Fig. 3a). Pathway enrichment analysis revealed that the metabolites correlated with PFASs exposure were primarily from mitochondrial metabolism, kynurenine, eicosanoid, glycolysis, niacin, bioamine and neurotransmitter metabolism (Fig. S3).

We next used multiple linear regression models to further confirm the relationship between PFASs exposure and metabolic disturbances in COVID-19 patients. After controlling for the confounding variables, the associations between ∑ (12) PFASs and urine endogenous metabolites from the metabolic pathways of kynurenine and eicosanoid and mitochondrial metabolism remained statistically significant (Fig. 3b). Similar associations were observed for PFOS and PFOA with urine metabolites in COVID-19 patients (Figs. S3 and S4). In detail, we observed three major patterns: (i) 13 PFASs-associated urine metabolites were identified to be produced or largely regulated by mitochondrial function (Fig. 3b); (ii) We identified novel positive associations between urinary PFASs and multiple key metabolites in kynurenine metabolism including kynurenine, 3-hydroxyanthranilic acid, hydroxykynurenine, and N-formylkynurenine with the combined β coefficient of 0.60 [95% CI: 0.25–0.95, $P = 0.001$] after adjusting for confounding variables (Fig. 3b); and (iii) PFOS, PFOA and ∑ (12) PFASs were all positively correlated with eicosanoids, which are bioactive lipid mediators involved in immune and inflammatory responses (combined β coefficient of 0.24 [95% CI: 0.16–0.32, $P < 0.001$] for total PFASs after confounders adjustment) (Fig. 3b, Figs. S4 and S5). The interconnections of metabolites and their metabolic pathways associated with PFASs exposure in COVID-19 patients are summarized in Fig. 3c. Interestingly, metabolic dysregulation of PFASs-associated metabolites and biochemical pathways were also reported to be connected to disease pathogenesis and the host defense response to COVID-19 infection (Ayres 2020).

3.6. The relationship between PFASs-associated urinary metabolites and clinical biomarkers of mitochondrial function and immune activity in COVID-19 patients

We next analyzed whether urinary metabolites associated with PFASs were also correlated with lab biomarkers for mitochondrial function and immune activity. Serum GDF-15 is a known biomarker of

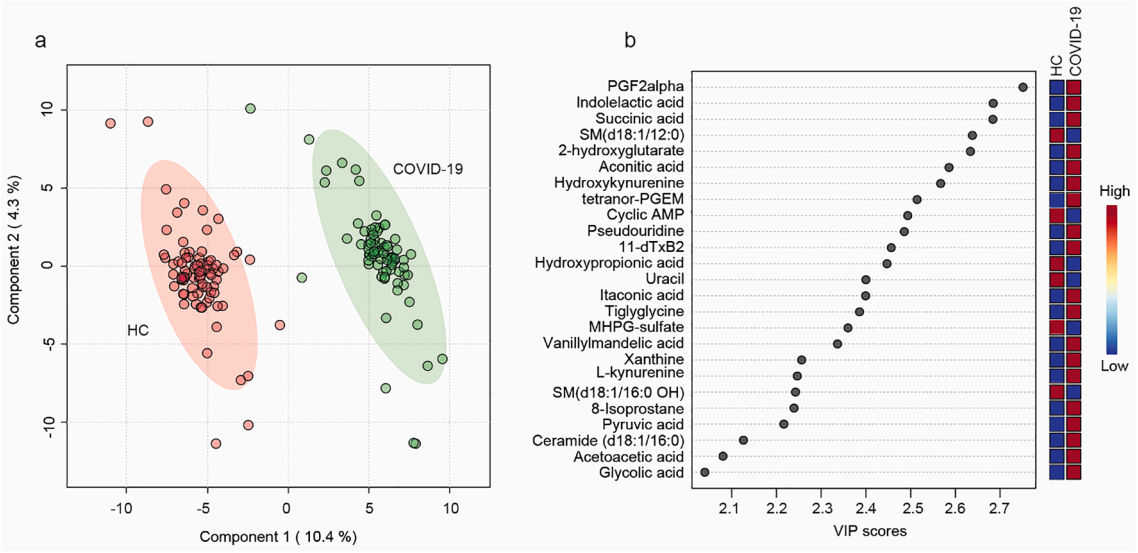

Fig. 2. Metabolomic analysis revealed distinct urinary metabolic profiles between symptom-free healthy controls (HC) and COVID-19 patients. (a) Partial least squares discriminant analysis (PLS-DA) plot showed the separation of urine metabolome between HC (n = 80) and COVID-19 patients (n = 80). (b) The top 25 differential metabolites between HC and COVID-19 revealed by variable importance in projection (VIP). Metabolites with VIP scores >1.5 were considered as significant towards the classification model.

mitochondrial function (Montero et al., 2016). We found that the levels of urinary metabolites in mitochondrial metabolism such as L-Acetylcarnitine, Aconitic acid, and hydroxypropionic acid correlated well with the concentration of serum GDF-15 (Spearman's rank correlation, all *P values* < 0.01 or 0.05) (Fig. 4a–c). Lymphocyte percentage (LYP, %) in whole blood is one of the indicators for the changes in immune function in COVID-19 patients (Tan et al., 2020). There were significant negative correlations between urinary metabolites from kynurenine pathway and LYP (Fig. 4d–f).

4. Discussion

The potential interactions between environmental toxicants exposure and COVID-19 remain largely unknown. This study represented the first attempt to explore the associations between PFASs in urine and COVID-19 susceptibility. Our results indicate increased risks for COVID-19 infection with high urinary PFASs after adjusting for potential confounding factors including age, gender, number of diabetes, CVDs, and urine albumin-to-creatinine ratio. Using metabolome-wide association analysis, we found that urinary endogenous metabolites associated with PFASs are involved in essential metabolic pathways underlying the pathophysiology of COVID-19 infection including mitochondrial metabolism, eicosanoids, and kynurenine pathways (Fig. 3c).

Since 2014, China has become the exclusive producer and supplier of PFOS globally, and the largest producer of PFOA in the world. Both Shandong and Shanxi provinces had relatively high industrial emission of PFASs in China. It is not a surprise that we detected PFOS and PFOA in the urine of all subjects. There is no previously published data for PFASs exposure from the same regions. However, the urinary levels of PFOS and PFOA we measured in our study were dramatically higher than the values reported in 2014 in the general population of Tianjin (Zhang et al., 2015). Out of 12 common PFASs measured in our study, the associations with COVID-19 infection are significant for PFOS, PFOA, and total PFASs after adjustment for confounders. Urinary PFOS and PFOA are highly correlated, which could likely lead to the positive associations observed for both PFOS and PFOA on COVID susceptibility. This observation highlighted the needs to treat PFASs as a class of chemicals rather than individual chemical (Cousins et al., 2020; Kwiatkowski et al., 2020).

Urine is the biological fluid of choice in our study because of the ease of collection, and unlike blood, it contains rich information on the functionality of organs at the metabolic level and provides an integrated estimate of exposure overtime, making it valuable for a broad range of biological investigations (Miller et al., 2019). Regarding PFASs, according to the outcomes of animal studies, urine is the major excretion route for PFOA and PFOS in rats (Cui et al., 2010). A human study reported that for all PFASs except PFUnA, levels in urine correlated positively with levels in the blood (Zhang et al., 2013). Consistent with the previous study, we also identified significant correlations between serum and the corresponding urine PFOS and PFOA concentrations in our cohort. Together, these findings suggest that urinary concentrations might be good indicators of the internal dose for PFASs, and this less invasive strategy can therefore be used in future epidemiological and biomonitoring studies. However, it is worth mentioning that urinary PFASs might be influenced by kidney function. Those who had higher and longer exposure might have impaired kidney function and thus cause larger variation in urinary PFASs levels than those in serum (Lin et al., 2021). Our urine metabolomics, in combination with metabolome-wide association analysis, identified a strong urine metabolic signature associated with PFASs exposure in COVID-19 patients, which can be traced to altered mitochondrial regulation of cellular redox, signaling, and energy. Mitochondria have been considered as a nexus point for the convergence of environmental stress signaling (Youle and van der Bliek 2012). In our study, we found that both Krebs cycle-related metabolites (succinic acid, pyruvic acid, and aconitic acid) produced by mitochondria and acylcarnitines (acetylcarnitine and butyrylcarnitine) involved in fatty acid oxidation in mitochondria were positively associated with PFASs exposure. Similarly, the urinary levels of these intermediate metabolites in mitochondrial metabolism were also found to be associated with other environmental stressors, including fine particulate matter air pollution ($PM_{2.5}$) (Chen et al., 2019), heavy metals (Al-Madani et al., 2010), and respiratory syncytial virus infection (Turi et al., 2018). The accumulation of succinic acid and acylcarnitines may induce mitochondrial reactive oxygen species (ROS) generation and cause tissue injury (Muoio and Neufer 2012; Zhang et al., 2020b).

Our study demonstrated positive associations between PFASs exposure and several key metabolites (L-Kynurenine, 3-hydroxyanthranilic acid, hydroxykynurenine, and N-formylkynurenine) in the kynurenine pathway, independent of confounders. The kynurenine pathway is

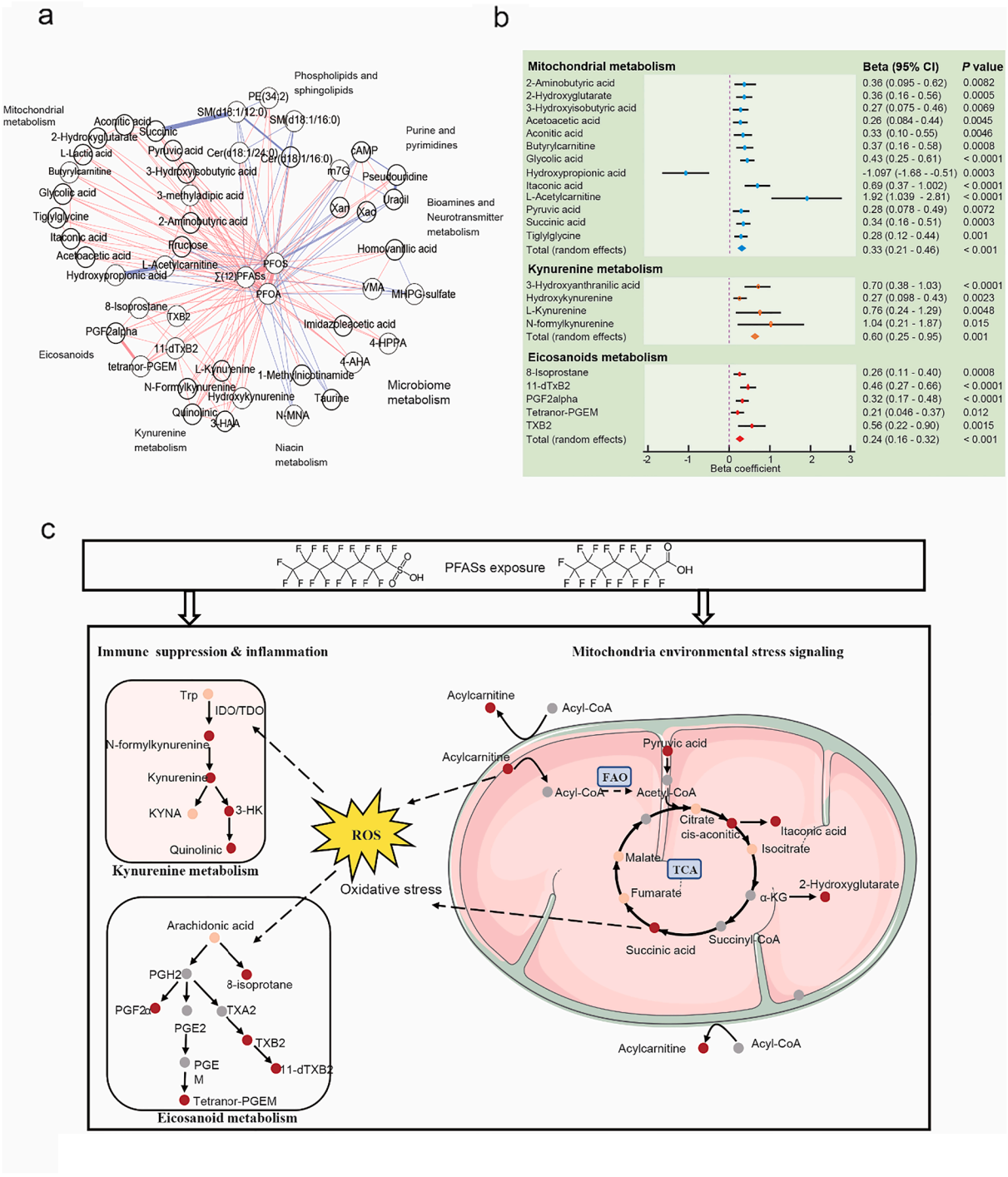

Fig. 3. Altered mitochondrial metabolism and increased urinary metabolites in the pathways of kynurenine and eicosanoids metabolism are associated with elevated PFASs in COVID-19 patients. (a) Urinary endogenous metabolites-PFASs association analysis. The metabolites that are significantly different between unhealthy controls (HC) and COVID-19 patients (VIP scores > 1.5 in PLS-DA) were used for the analysis. Data were log 2 transformed, and Spearman's rank correlation was performed. The correlation threshold was set as 0.2 and P value ≤ 0.05. Edge color indicates a positive (red) or inverse (blue) correlation. (b) Multiple linear regression models were used to confirm the adjusted associations between PFASs exposure and altered urinary metabolites in COVID-19 patients. Z scores of Σ (12) PFASs were calculated, and urinary endogenous metabolites were log 2 transformed before analysis. The effect sizes (Beta) and P values were adjusted for age, gender, body mass index (BMI), diabetes, cardiovascular diseases (CVDs), and urine albumin-to-creatinine ratio (UACR). The combined effect of PFASs exposure on a metabolic pathway was *meta*-analyzed using the random-effects model. (c) The summary of metabolic dysregulations associated with PFASs exposure in COVID-19 patients. The red dots indicate the metabolites with significant positive associations with total PFASs in adjusted multiple linear regression models, while the pink dots were the metabolites without significant associations with PFASs. The gray dots are the metabolites that were not detected or targeted. Abbreviations: PFOS: Perfluorooctanesulfonic acid; PFOA: Perfluorooctanoic acid; 3-HAA: 3-Hydroxyanthranilic acid; N-MNA: N-Methylnicotinamide; 4-AHA: 4-Aminohippuric acid; VMA: Vanillylmandelic acid; Xao: Xanthosine; Xan: Xanthine; m7G: 7-Methylguanosine; Cer: Ceramide; BMI: body mass index; CVD: cardiovascular disease; WBC: white blood cells; RBCs: red blood cells; ROS: reactive oxygen species; TCA: tricarboxylic acid cycle; FAO: fatty acid oxidation. (For interpretation of the references to color in this figure legend, the reader is referred to the web version of this article.)

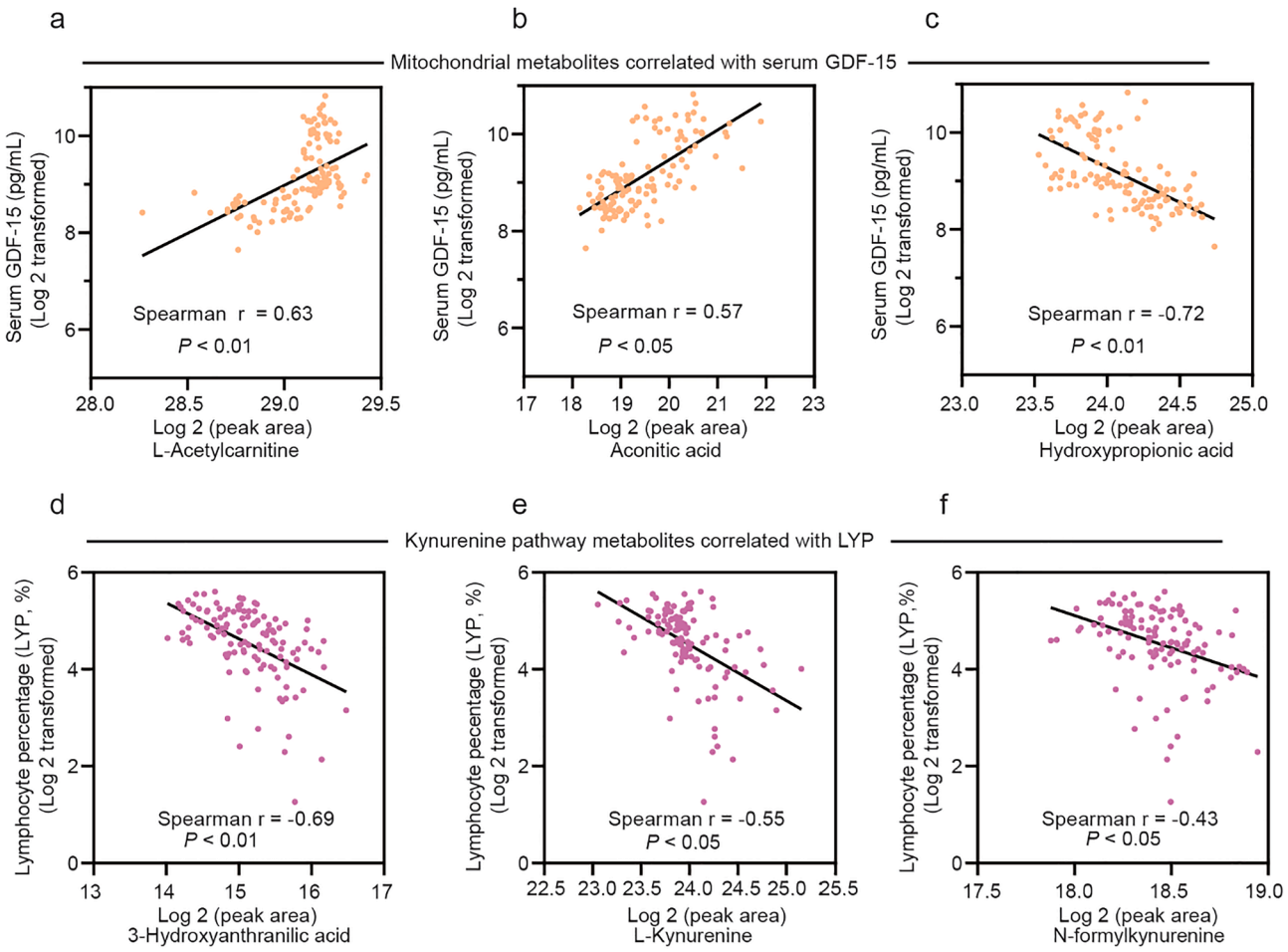

Fig. 4. Metabolites correlated to clinical biomarkers for mitochondrial function and immune responses. (a–c) Urinary metabolites levels in mitochondrial metabolism were correlated with serum growth differentiation factor-15 (GDF-15), a biomarker for mitochondrial function. (d–f) Kynurenine pathway metabolites had significant correlations with measurements of immune response biomarker, lymphocyte percentage (LYP). Data were log 2 transformed and Spearman's rank correlation was conducted. Spearman's correlation coefficient r and *P* values were reported.

highly regulated in the immune system, where it promotes immunosuppression in response to inflammation or infection (Cervenka et al., 2017). For example, the accumulation of kynurenine and hydroxykynurenine inhibits T-cell proliferation at G1 phase and induces natural killer cells apoptosis (Wu et al., 2018). The immunotoxic effects of PFASs had been previously implicated in several epidemiological studies of childhood immunization (Grandjean et al., 2012; Grandjean et al., 2017), in which high PFASs exposure was correlated with decreased immune responses to childhood vaccines. Importantly, alteration of kynurenine metabolism was also observed in a recent serum metabolomic analysis of COVID-19 patients (Thomas et al., 2020). Eicosanoids, including prostaglandins, thromboxanes, and isoprostanes, are bioactive lipid mediators derived from polyunsaturated fatty acids (PUFAs). Eicosanoid signaling, similar to cytokine signaling, regulates a diverse set of inflammatory processes, primarily as a pro-inflammatory component of the innate immune responses (Dennis and Norris 2015). Here, we observed, for the first time, that increased levels of eicosanoids were associated with elevated PFASs exposure.

Our study has several limitations. First, our study is limited by the small sample size. Future studies are warranted to confirm the findings in large cohorts. Second, even though the controls were tested negative for SARS-CoV-2 through nasopharyngeal swab nucleic acid amplification, we can not completely exclude the potential false negative results of PCR testing. Third, the observational nature of the study precludes inferences of causality. PFAS-associated metabolic signatures in urine should be interpreted as potential biomarkers rather than causal mechanisms of PFASs exposure. Finally, COVID-19 is a new public concern. The possibility of residual confounding from unknown variables cannot be excluded.

In summary, we observed significantly higher risks of SARS-CoV-2 infection in the subjects with increased urinary PFOS, PFOA, and total PFASs. PFASs exposure in COVID-19 patients are associated with the metabolic disturbances in biochemical pathways involved in mitochondria stress signaling and the regulation of immune function, including fatty acid oxidation, TCA cycle, eicosanoid, and kynurenine pathways. Our study suggests a new risk factor for susceptibility to COVID-19, in addition to older age, male sex and the presence of cardiometabolic/vascular comorbidities. Further research should integrate experimental and epidemiological approaches to elucidate the underlying mechanisms of PFASs exposure in COVID-19 infection.

Funding

This study was supported by Natural Science Foundation of Shanxi Province (201901D221113), Natural Science Foundation of Shandong Province (ZR2017MH075), and a special grant for COVID-19 prevention and control from Department of Education, Shanxi Province. The sponsor had no role in design and conduct of the study; collection, management, analysis, and interpretation of the data; preparation, review, or approval of the manuscript; and decision to submit the manuscript for publication.

Declaration of Competing Interest

The authors declare that they have no known competing financial interests or personal relationships that could have appeared to influence the work reported in this paper.

Appendix A. Supplementary material

Supplementary data to this article can be found online at https://doi.org/10.1016/j.envint.2021.106524.

References

Ait Bamai, Y., Goudarzi, H., Araki, A., Okada, E., Kashino, I., Miyashita, C., Kishi, R., 2020. Effect of prenatal exposure to per- and polyfluoroalkyl substances on childhood allergies and common infectious diseases in children up to age 7 years: The Hokkaido study on environment and children's health. Environ. Int. 143, 105979 https://doi.org/10.1016/j.envint.2020.105979.

Al-Madani, W.A., Siddiqi, N.J., Alhomida, A.S., Khan, H.A., Arif, I.A., Kishore, U., 2010. Increased urinary excretion of carnitine and acylcarnitine by mercuric chloride is reversed by 2,3-dimercapto-1-propanesulfonic acid in rats. Int. J. Toxicol. 29, 313–317. https://doi.org/10.1177/1091581810364852.

Alderete, T.L., Jin, R., Walker, D.I., Valvi, D., Chen, Z., Jones, D.P., Peng, C., Gilliland, F. D., Berhane, K., Conti, D.V., Goran, M.I., Chatzi, L., 2019. Perfluoroalkyl substances, metabolomic profiling, and alterations in glucose homeostasis among overweight and obese Hispanic children: A proof-of-concept analysis. Environ. Int. 126, 445–453. https://doi.org/10.1016/j.envint.2019.02.047.

Anastassopoulou, C., Gkizarioti, Z., Patrinos, G.P., Tsakris, A., 2020. Human genetic factors associated with susceptibility to SARS-CoV-2 infection and COVID-19 disease severity. Hum. Genomics 14, 40. https://doi.org/10.1186/s40246-020-00290-4.

Aung, N., Khanji, M.Y., Munroe, P.B., Petersen, S.E., 2020. Causal Inference for Genetic Obesity, Cardiometabolic Profile and COVID-19 Susceptibility: A Mendelian Randomization Study. Front. Genet. 11, 586308 https://doi.org/10.3389/fgene.2020.586308.

Ayres, J.S., 2020. A metabolic handbook for the COVID-19 pandemic. Nat. Metab. 2, 572–585. https://doi.org/10.1038/s42255-020-0237-2.

Cervenka, I., Agudelo, L.Z., Ruas, J.L., 2017. Kynurenines: Tryptophan's metabolites in exercise, inflammation, and mental health. Science 357, eaaf9794. https://doi.org/10.1126/science.aaf9794.

Chang, E.T., Adami, H.O., Boffetta, P., Wedner, H.J., Mandel, J.S., 2016. A critical review of perfluorooctanoate and perfluorooctanesulfonate exposure and immunological health conditions in humans. Crit. Rev. Toxicol. 46, 279–331. https://doi.org/10.3109/10408444.2015.1122573.

Chen, C., Li, H., Niu, Y., Liu, C., Lin, Z., Cai, J., Li, W., Ge, W., Chen, R., Kan, H., 2019. Impact of short-term exposure to fine particulate matter air pollution on urinary metabolome: A randomized, double-blind, crossover trial. Environ. Int. 130, 104878 https://doi.org/10.1016/j.envint.2019.05.072.

Cousins, I.T., DeWitt, J.C., Gluge, J., Goldenman, G., Herzke, D., Lohmann, R., Ng, C.A., Scheringer, M., Wang, Z., 2020. The high persistence of PFAS is sufficient for their management as a chemical class. Environ. Sci. Process Impacts 22, 2307–2312. https://doi.org/10.1039/d0em00355g.

Cui, L., Liao, C.Y., Zhou, Q.F., Xia, T.M., Yun, Z.J., Jiang, G.B., 2010. Excretion of PFOA and PFOS in male rats during a subchronic exposure. Arch. Environ. Contam. Toxicol. 58, 205–213. https://doi.org/10.1007/s00244-009-9336-5.

Dennis, E.A., Norris, P.C., 2015. Eicosanoid storm in infection and inflammation. Nat. Rev. Immunol. 15, 511–523. https://doi.org/10.1038/nri3859.

DeWitt, J.C., Blossom, S.J., Schaider, L.A., 2019. Exposure to per-fluoroalkyl and polyfluoroalkyl substances leads to immunotoxicity: epidemiological and toxicological evidence. J. Expo. Sci. Environ. Epidemiol. 29, 148–156. https://doi.org/10.1038/s41370-018-0097-y.

Ganeshan, K., Chawla, A., 2014. Metabolic regulation of immune responses. Annu. Rev. Immunol. 32, 609–634. https://doi.org/10.1146/annurev-immunol-032713-120236.

Gonzalez Plaza, J.J., Hulak, N., Kausova, G., Zhumadilov, Z., Akilzhanova, A., 2016. Role of metabolism during viral infections, and crosstalk with the innate immune system. Intractable Rare Dis. Res. 5, 90–96. https://doi.org/10.5582/irdr.2016.01008.

Grandjean, P., Andersen, E.W., Budtz-Jorgensen, E., Nielsen, F., Molbak, K., Weihe, P., Heilmann, C., 2012. Serum vaccine antibody concentrations in children exposed to perfluorinated compounds. JAMA 307, 391–397. https://doi.org/10.1001/jama.2011.2034.

Grandjean, P., Heilmann, C., Weihe, P., Nielsen, F., Mogensen, U.B., Timmermann, A., Budtz-Jorgensen, E., 2017. Estimated exposures to perfluorinated compounds in infancy predict attenuated vaccine antibody concentrations at age 5-years. J. Immunotoxicol. 14, 188–195. https://doi.org/10.1080/1547691X.2017.1360968.

Granum, B., Haug, L.S., Namork, E., Stolevik, S.B., Thomsen, C., Aaberge, I.S., van Loveren, H., Lovik, M., Nygaard, U.C., 2013. Pre-natal exposure to perfluoroalkyl substances may be associated with altered vaccine antibody levels and immune-related health outcomes in early childhood. J. Immunotoxicol. 10, 373–379. https://doi.org/10.3109/1547691X.2012.755580.

Haitao, T., Vermunt, J.V., Abeykoon, J., Ghamrawi, R., Gunaratne, M., Jayachandran, M., Narang, K., Parashuram, S., Suvakov, S., Garovic, V.D., 2020. COVID-19 and sex differences: mechanisms and biomarkers. Mayo Clin. Proc. 95, 2189–2203. https://doi.org/10.1016/j.mayocp.2020.07.024.

Han, J., Xia, Y., Lin, L., Zhang, Z., Tian, H., Li, K., 2018. Next-generation metabolomics in the development of new antidepressants: using albiflorin as an example. Curr. Pharm. Des. 24, 2530–2540. https://doi.org/10.2174/1381612824666180727114134.

Harel, O., Perkins, N., Schisterman, E.F., 2014. The use of multiple imputation for data subject to limits of detection. Sri. Lankan J. Appl. Stat. 5, 227–246. https://doi.org/10.4038/sljastats.v5i4.7792.

Impinen, A., Nygaard, U.C., Lodrup Carlsen, K.C., Mowinckel, P., Carlsen, K.H., Haug, L. S., Granum, B., 2018. Prenatal exposure to perfluoralkyl substances (PFASs) associated with respiratory tract infections but not allergy- and asthma-related health outcomes in childhood. Environ. Res. 160, 518–523. https://doi.org/10.1016/j.envres.2017.10.012.

Jung, C.Y., Park, H., Kim, D.W., Lim, H., Chang, J.H., Choi, Y.J., Kim, S.W., Chang, T.I., 2020. Association between body mass index and risk of COVID-19: A nationwide case-control study in South Korea. Clin. Infect. Dis. ciaa1257 https://doi.org/10.1093/cid/ciaa1257.

Khamis, M.M., Holt, T., Awad, H., El-Aneed, A., Adamko, D.J., 2018. Comparative analysis of creatinine and osmolality as urine normalization strategies in targeted metabolomics for the differential diagnosis of asthma and COPD. Metabolomics 14, 115. https://doi.org/10.1007/s11306-018-1418-9.

Kielsen, K., Shamim, Z., Ryder, L.P., Nielsen, F., Grandjean, P., Budtz-Jorgensen, E., Heilmann, C., 2016. Antibody response to booster vaccination with tetanus and diphtheria in adults exposed to perfluorinated alkylates. J. Immunotoxicol. 13, 270–273. https://doi.org/10.3109/1547691X.2015.1067259.

Kingsley, S.L., Walker, D.I., Calafat, A.M., Chen, A., Papandonatos, G.D., Xu, Y., Jones, D. P., Lanphear, B.P., Pennell, K.D., Braun, J.M., 2019. Metabolomics of childhood exposure to perfluoroalkyl substances: a cross-sectional study. Metabolomics 15, 95. https://doi.org/10.1007/s11306-019-1560-z.

Kwiatkowski, C.F., Andrews, D.Q., Birnbaum, L.S., Bruton, T.A., DeWitt, J.C., Knappe, D. R.U., Maffini, M.V., Miller, M.F., Pelch, K.E., Reade, A., Soehl, A., Trier, X., Venier, M., Wagner, C.C., Wang, Z.Y., Blum, A., 2020. Scientific basis for managing PFAS as a chemical class. Environ. Sci. Tech. Let. 7, 532–543. https://doi.org/10.1021/acs.estlett.0c00255.

Li, J., Guo, F., Wang, Y., Zhang, J., Zhong, Y., Zhao, Y., Wu, Y., 2013. Can nail, hair and urine be used for biomonitoring of human exposure to perfluorooctane sulfonate and perfluorooctanoic acid? Environ. Int. 53, 47–52. https://doi.org/10.1016/j.envint.2012.12.002.

Li, P., Oyang, X., Zhao, Y., Tu, T., Tian, X., Li, L., Zhao, Y., Li, J., Xiao, Z., 2019. Occurrence of perfluorinated compounds in agricultural environment, vegetables, and fruits in regions influenced by a fluorine-chemical industrial park in China. Chemosphere 225, 659–667. https://doi.org/10.1016/j.chemosphere.2019.03.045.

Lin, P.D., Cardenas, A., Hauser, R., Gold, D.R., Kleinman, K.P., Hivert, M.F., Calafat, A. M., Webster, T.F., Horton, E.S., Oken, E., 2021. Per- and polyfluoroalkyl substances and kidney function: Follow-up results from the Diabetes Prevention Program trial. Environ. Int. 148, 106375 https://doi.org/10.1016/j.envint.2020.106375.

Liu, T., Liang, W., Zhong, H., He, J., Chen, Z., He, G., Song, T., Chen, S., Wang, P., Li, J., Lan, Y., Cheng, M., Huang, J., Niu, J., Xia, L., Xiao, J., Hu, J., Lin, L., Huang, Q., Rong, Z., Deng, A., Zeng, W., Li, J., Li, X., Tan, X., Kang, M., Guo, L., Zhu, Z., Gong, D., Chen, G., Dong, M., Ma, W., 2020. Risk factors associated with COVID-19 infection: a retrospective cohort study based on contacts tracing. Emerg. Microbes Infect. 9, 1546–1553. https://doi.org/10.1080/22221751.2020.1787799.

Liu, Z., Lu, Y., Song, X., Jones, K., Sweetman, A.J., Johnson, A.C., Zhang, M., Lu, X., Su, C., 2019. Multiple crop bioaccumulation and human exposure of perfluoroalkyl substances around a mega fluorochemical industrial park, China: Implication for planting optimization and food safety. Environ. Int. 127, 671–684. https://doi.org/10.1016/j.envint.2019.04.008.

Lopez-Giacoman, S., Madero, M., 2015. Biomarkers in chronic kidney disease, from kidney function to kidney damage. World J. Nephrol. 4, 57–73. https://doi.org/10.5527/wjn.v4.i1.57.

Lubin, J.H., Colt, J.S., Camann, D., Davis, S., Cerhan, J.R., Severson, R.K., Bernstein, L., Hartge, P., 2004. Epidemiologic evaluation of measurement data in the presence of detection limits. Environ. Health Perspect. 112, 1691–1696. https://doi.org/10.1289/ehp.7199.

McGlinchey, A., Sinioja, T., Lamichhane, S., Sen, P., Bodin, J., Siljander, H., Dickens, A. M., Geng, D., Carlsson, C., Duberg, D., Ilonen, J., Virtanen, S.M., Dirven, H., Berntsen, H.F., Zimmer, K., Nygaard, U.C., Oresic, M., Knip, M., Hyotylainen, T., 2020. Prenatal exposure to perfluoroalkyl substances modulates neonatal serum phospholipids, increasing risk of type 1 diabetes. Environ. Int. 143, 105935 https://doi.org/10.1016/j.envint.2020.105935.

Michaudel, C., Sokol, H., 2020. The Gut Microbiota at the service of immunometabolism. Cell Metab. 32, 514–523. https://doi.org/10.1016/j.cmet.2020.09.004.

Miller, I.J., Peters, S.R., Overmyer, K.A., Paulson, B.R., Westphall, M.S., Coon, J.J., 2019. Real-time health monitoring through urine metabolomics. NPJ Digit. Med. 2, 109. https://doi.org/10.1038/s41746-019-0185-y.

Montero, R., Yubero, D., Villarroya, J., Henares, D., Jou, C., Rodriguez, M.A., Ramos, F., Nascimento, A., Ortez, C.I., Campistol, J., Perez-Duenas, B., O'Callaghan, M., Pineda, M., Garcia-Cazorla, A., Oferil, J.C., Montoya, J., Ruiz-Pesini, E., Emperador, S., Meznaric, M., Campderros, L., Kalko, S.G., Villarroya, F., Artuch, R., Jimenez-Mallebrera, C., 2016. GDF-15 is elevated in children with mitochondrial diseases and is induced by mitochondrial dysfunction. PLoS ONE 11, e0148709. https://doi.org/10.1371/journal.pone.0148709.

Muoio, D.M., Neufer, P.D., 2012. Lipid-induced mitochondrial stress and insulin action in muscle. Cell Metab. 15, 595–605. https://doi.org/10.1016/j.cmet.2012.04.010.

Oresic, M., McGlinchey, A., Wheelock, C.E., Hyotylainen, T., 2020. Metabolic signatures of the exposome-quantifying the impact of exposure to environmental chemicals on human health. Metabolites 10, 454. https://doi.org/10.3390/metabo10110454.

Pan, Y., Shi, Y., Wang, J., Cai, Y., Wu, Y., 2010. Concentrations of perfluorinated compounds in human blood from twelve cities in China. Environ. Toxicol. Chem. 29, 2695–2701. https://doi.org/10.1002/etc.342.

Pelch, K.E., Reade, A., Wolffe, T.A.M., Kwiatkowski, C.F., 2019. PFAS health effects database: Protocol for a systematic evidence map. Environ. Int. 130, 104851 https://doi.org/10.1016/j.envint.2019.05.045.

Perez, F., Nadal, M., Navarro-Ortega, A., Fabrega, F., Domingo, J.L., Barcelo, D., Farre, M., 2013. Accumulation of perfluoroalkyl substances in human tissues. Environ. Int. 59, 354–362. https://doi.org/10.1016/j.envint.2013.06.004.

Shahfiza, N., Osman, H., Hock, T.T., Abdel-Hamid, A.Z., 2017. Metabolomics approach for multibiomarkers determination to investigate dengue virus infection in human patients. Acta Biochim. Pol. 64.

Shen, B., Yi, X., Sun, Y., Bi, X., Du, J., Zhang, C., Quan, S., Zhang, F., Sun, R., Qian, L., Ge, W., Liu, W., Liang, S., Chen, H., Zhang, Y., Li, J., Xu, J., He, Z., Chen, B., Wang, J., Yan, H., Zheng, Y., Wang, D., Zhu, J., Kong, Z., Kang, Z., Liang, X., Ding, X., Ruan, G., Xiang, N., Cai, X., Gao, H., Li, L., Li, S., Xiao, Q., Lu, T., Zhu, Y., Liu, H., Chen, H., Guo, T., 2020. Proteomic and metabolomic characterization of COVID-19 patient sera. Cell 182, 59–72. https://doi.org/10.1016/j.cell.2020.05.032.

Susmann, H.P., Schaider, L.A., Rodgers, K.M., Rudel, R.A., 2019. Dietary Habits Related to food packaging and population exposure to PFASs. Environ. Health Perspect. 127, 107003 https://doi.org/10.1289/EHP4092.

Tan, L., Wang, Q., Zhang, D., Ding, J., Huang, Q., Tang, Y.Q., Wang, Q., Miao, H., 2020. Lymphopenia predicts disease severity of COVID-19: a descriptive and predictive study. Signal Transduct. Target Ther. 5, 33. https://doi.org/10.1038/s41392-020-0148-4.

Thomas, T., Stefanoni, D., Reisz, J.A., Nemkov, T., Bertolone, L., Francis, R.O., Hudson, K.E., Zimring, J.C., Hansen, K.C., Hod, E.A., Spitalnik, S.L., D'Alessandro, A., 2020. COVID-19 infection alters kynurenine and fatty acid metabolism, correlating with IL-6 levels and renal status. JCI Insight 5, e140327. https://doi.org/10.1172/jci.insight.140327.

Tian, Y., Zhou, Y., Miao, M., Wang, Z., Yuan, W., Liu, X., Wang, X., Wang, Z., Wen, S., Liang, H., 2018. Determinants of plasma concentrations of perfluoroalkyl and polyfluoroalkyl substances in pregnant women from a birth cohort in Shanghai. China. Environ. Int. 119, 165–173. https://doi.org/10.1016/j.envint.2018.06.015.

Timmermann, C.A., Budtz-Jorgensen, E., Jensen, T.K., Osuna, C.E., Petersen, M.S., Steuerwald, U., Nielsen, F., Poulsen, L.K., Weihe, P., Grandjean, P., 2017. Association between perfluoroalkyl substance exposure and asthma and allergic disease in children as modified by MMR vaccination. J. Immunotoxicol. 14, 39–49. https://doi.org/10.1080/1547691X.2016.1254306.

Turi, K.N., Romick-Rosendale, L., Gebretsadik, T., Watanabe, M., Brunwasser, S., Anderson, L.J., Moore, M.L., Larkin, E.K., Peebles Jr., R.S., Hartert, T.V., 2018. Using urine metabolomics to understand the pathogenesis of infant respiratory syncytial virus (RSV) infection and its role in childhood wheezing. Metabolomics 14, 135. https://doi.org/10.1007/s11306-018-1431-z.

Viner, R.M., Mytton, O.T., Bonell, C., Melendez-Torres, G.J., Ward, J., Hudson, L., Waddington, C., Thomas, J., Russell, S., van der Klis, F., Koirala, A., Ladhani, S., Panovska-Griffiths, J., Davies, N.G., Booy, R., Eggo, R.M., 2020. Susceptibility to SARS-CoV-2 infection among children and adolescents compared with adults: A systematic review and meta-analysis. JAMA Pediatr. 175, 143–156. https://doi.org/10.1001/jamapediatrics.2020.4573.

Wang, Q., Ruan, Y., Lin, H., Lam, P.K.S., 2020. Review on perfluoroalkyl and polyfluoroalkyl substances (PFASs) in the Chinese atmospheric environment. Sci. Total Environ. 737, 139804 https://doi.org/10.1016/j.scitotenv.2020.139804.

Wu, H., Gong, J., Liu, Y., 2018. Indoleamine 2, 3-dioxygenase regulation of immune response (Review). Mol. Med. Rep. 17, 4867–4873. https://doi.org/10.3892/mmr.2018.8537.

Xie, S., Wang, T., Liu, S., Jones, K.C., Sweetman, A.J., Lu, Y., 2013. Industrial source identification and emission estimation of perfluorooctane sulfonate in China. Environ. Int. 52, 1–8. https://doi.org/10.1016/j.envint.2012.11.004.

Xing, Y., Wong, G.W.K., Ni, W., Hu, X., Xing, Q., 2020. Rapid response to an outbreak in Qingdao. China. N. Engl. J. Med. 383, e129 https://doi.org/10.1056/NEJMc2032361.

Youle, R.J., van der Bliek, A.M., 2012. Mitochondrial fission, fusion, and stress. Science 337, 1062–1065. https://doi.org/10.1126/science.1219855.

Yuan, M., Breitkopf, S.B., Yang, X., Asara, J.M., 2012. A positive/negative ion-switching, targeted mass spectrometry-based metabolomics platform for bodily fluids, cells, and fresh and fixed tissue. Nat. Protoc. 7, 872–881. https://doi.org/10.1038/nprot.2012.024.

Zeng, Z., Song, B., Xiao, R., Zeng, G., Gong, J., Chen, M., Xu, P., Zhang, P., Shen, M., Yi, H., 2019. Assessing the human health risks of perfluorooctane sulfonate by in vivo and in vitro studies. Environ. Int. 126, 598–610. https://doi.org/10.1016/j.envint.2019.03.002.

Zhang, T., Sun, H., Qin, X., Gan, Z., Kannan, K., 2015. PFOS and PFOA in paired urine and blood from general adults and pregnant women: assessment of urinary elimination. Environ. Sci. Pollut. Res. Int. 22, 5572–5579. https://doi.org/10.1007/s11356-014-3725-7.

Zhang, X., Rao, H., Wu, Y., Huang, Y., Dai, H., 2020a. Comparison of spatiotemporal characteristics of the COVID-19 and SARS outbreaks in mainland China. BMC Infect. Dis. 20, 805. https://doi.org/10.1186/s12879-020-05537-y.

Zhang, Y., Beesoon, S., Zhu, L., Martin, J.W., 2013. Biomonitoring of perfluoroalkyl acids in human urine and estimates of biological half-life. Environ. Sci. Technol. 47, 10619–10627. https://doi.org/10.1021/es401905e.

Zhang, Y., Zhang, M., Zhu, W., Yu, J., Wang, Q., Zhang, J., Cui, Y., Pan, X., Gao, X., Sun, H., 2020b. Succinate accumulation induces mitochondrial reactive oxygen species generation and promotes status epilepticus in the kainic acid rat model. Redox Biol. 28, 101365 https://doi.org/10.1016/j.redox.2019.101365.

Zhu, N., Zhang, D., Wang, W., Li, X., Yang, B., Song, J., Zhao, X., Huang, B., Shi, W., Lu, R., Niu, P., Zhan, F., Ma, X., Wang, D., Xu, W., Wu, G., Gao, G.F., Tan, W., 2020. A novel coronavirus from patients with pneumonia in China, 2019. N. Engl. J. Med. 382, 727–733. https://doi.org/10.1056/NEJMoa2001017.